Textile-Only Capacitive Sensors for Facile Fabric Integration without Compromise of Wearability

Qi Zhang, Yu Lu Wang, Yun Xia, Peng Fei Zhang, Timothy V. Kirk, and Xiao Dong Chen**

Wearable sensors promise advances in monitoring for athletes and patients, and offer the possibility of convenient longitudinal data collection without compromising lifestyle or comfort. To fully realize these possibilities, devices should be easily integrated into the clothing, accessories, and medical products that best suit consumers. An effective capacitive strain sensor whose components consist solely of fibers with a textile thread-like morphology, i.e., that requires no solid polymer matrix that complicates integration, and can be woven directly into the fabric of clothing, bandages, and other products is presented. It is produced by twisting two core-spun yarns into a fine double-ply yarn. The core-spun yarns are fabricated by wrapping silver-coated nylon fibers with cotton fibers, and fixing them with polyurethane. Excellent capacitive linearity is displayed, with high dielectric stability over 10 000 cycles of endurance testing. Other detection properties are in line with existing sensors, though with lower ultimate strain and elastic limit. Textile integration is demonstrated via incorporation with kneepads and gloves without compromise of comfort or range of motion. All materials are compatible with medical sterilization methods. Additional versatility is illustrated by weaving the core-spun yarn into pressure sensor arrays, which can be blended into wearable fabrics.

1. Introduction

Wearable sensors have been proposed for applications as diverse as monitoring athletic respiration,[1] facilitating human–machine interaction,[2] and long-term continuous monitoring of surgical recovery[3] or degenerative disease progression in longitudinal clinical studies.[4] To enable this range, electronic textile-based strain and pressure sensors have been applied to uses including human motion detection,[5–10] respiratory monitoring,[1,11] and tactile sensing.[12–15]

To maximize their utility, sensor systems should fulfil a number of technical and ergonomic criteria. These include signal stability and linearity, lack of hysteresis, and sufficient response time, on the electronic side.[16,17] Mechanical and comfort criteria include durability, long-term wearability, from skin-feel and sufficient extensibility and compliance, and ease of integration into preferred garments, accessories, or supports. Ultimately, a sensor should disappear into the most suitable consumer or medical product.

Textile-based sensors are typically divided into resistive[2,5–10,18–21] and capacitive[1,11–15] types. Compared with capacitive sensors, especially in strain-sensing applications, resistive sensors have several drawbacks: obvious hysteresis,[2,18–24] nonlinearity,[2,5–7,18–25] and poor stability from irreversible destruction of the conductive structure during repeated cycles of strain.[2,5,6,20–22,24,26–28] To minimize these issues, resistive elements have been used as electrodes of capacitive sensors, rather than as resistive sensors directly,[22,29–33] with these systems displaying fast response, linearity, and stability.[34,35]

Previously reported capacitive type textile-based sensors have mostly used woven or parallel plate capacitor structures. Here researchers wove shell-insulated conductive yarns,[14,15] or sandwiched dielectric layers between two conductive fabrics.[1,11,12] These sensors require sufficient surface area, described by the capacitance Equation (1), which is often fulfilled by embedding textile fibers in a planar polymer matrix.[15,35,36] This hinders integration with fabrics and clothing, especially when compared to textile-only sensors with thread-like morphology.[2,6,7] Further, these planar sensors' morphologies are often more suitable for pressure-sensing than strain-sensing applications.[1,11–15]

$$C = \varepsilon_0 \, \varepsilon_r \frac{A}{d} \tag{1}$$

Here C is capacitance, ε_0 and ε_r are the dielectric constant of a vacuum and the relative permittivity of dielectric media, respectively, A is area of electrodes, and d is thickness of the dielectric layer.

Q. Zhang, Prof. X. D. Chen
Department of Chemical and Biochemical Engineering
Xiamen University
No. 422, Siming South Road, Xiamen, Fujian Province 361005, China
E-mail: xdchen@mail.suda.edu.cn

Y. L. Wang
College of Energy
Xiamen University
No. 422, Siming South Road, Xiamen, Fujian Province 361005, China

Y. Xia, P. F. Zhang, Prof. T. V. Kirk, Prof. X. D. Chen
School of Chemical and Environmental Engineering
College of Chemistry
Chemical Engineering and Material Science
Soochow University
Suzhou Industrial Park Campus, Jiangsu Province 215123, China
E-mail: tim@suda.edu.cn

The ORCID identification number(s) for the author(s) of this article can be found under https://doi.org/10.1002/admt.201900485.

DOI: 10.1002/admt.201900485

There are few reports of effective capacitive textile-based strain sensors, despite the extensive reviews of the field available.[16,17,36,37] Recently Atalay et al.[35] developed a comb-shaped textile and silicone capacitive strain sensor, with conductive knit fabric as electrode, and silicone elastomer matrix as dielectric. Typical of many wearable sensor materials, it was able to sustain strains of up to 50%. Again, this system displayed a planar morphology, and required Velcro mounting to integrate with clothing. Additionally, performance of the textile–silicone capacitive sensor under large numbers of repeated cycles was not reported.

We present a matrix-free, textile-only, effective and robust capacitive strain sensor, formed by double-ply yarn, with an elastic limit of ≈18.5% elongation. This yarn, with fabric thread-like morphology, was produced by twisting together two core-spun yarns into a double helix structure. Without the requirement of a large planar surface or polymer matrix, the double-ply yarn sensor can be fine in diameter (0.6 ± 0.05 mm), and embedded into fabrics by means of knitting, sewing, or weaving. Although this material is unable to sustain the >50% strains reported by other researchers, with its fabric thread-like form, it can be integrated such that it comprises only a small fraction of wearable products. When combined with lack of direct anchoring to the skin, the sensor only experiences relatively small strains (<14%), even during high flexion-angle motions. A caveat, however, is that this sensor is not intended for 1:1 measurement of skin strain, unless low strain activities are targeted.

The core-spun yarns were fabricated by wrapping silver-coated nylon fibers with cotton fibers, and fixing with polyurethane adhesive. The silver fibers and their coating were used as electrodes and dielectric layers of the capacitive type sensor, respectively. Aided by the polyurethane adhesive, the core-spun yarns provide robust dielectric layers, and form a stable capacitive structure, giving the double-ply yarn strain sensor its excellent performance and resilience. The sensor displayed high sensitivity, excellent linearity and durability within the strain limits of typical use, and low hysteresis, maintained after 10 000 cycles of endurance testing. Proof-of-principle devices were demonstrated by integrating the sensor with kneepads and gloves. Detected motions included walking, jumping, and finger wiggling, with subjects not encountering discomfort, or restricted motion. Additionally, core-spun yarns can also be woven into textile-based pressure sensors, showing good performance in sensitivity, and demonstrating potential antibacterial properties. Sensor-integrated wearable fabrics, and mats for tactile detection, are presented. Further, the materials are suitable for sterilization by gamma irradiation, or ethylene oxide treatment—the most common methods used for medical consumables.

To the best of our knowledge, this is the first report of a matrix-free, textile-only capacitive type sensor with fabric thread-like morphology.

2. Results and Discussion

Silver fibers, that consist of synthetic or natural fibers coated with silver, are mature commercial materials for electromagnetic shielding,[38,39] and antibacterial clothes.[40,41] In this study, silver-coated nylon fibers were used. **Figure 1** shows the side view and the cross-section scanning electron microscope (SEM) micrographs of the fibers. As shown in Figure 1, the yarn is composed of eleven silver fibers, and each fiber has a thickness of about 25 µm. From the cross-section in the red square in Figure 1b, the silver coating appears to be ≈4 to 5 µm thick, and of uniform consistency. The silver coating provides electrical conductivity and potential antibacterial properties, and the nylon fiber core provides elasticity.

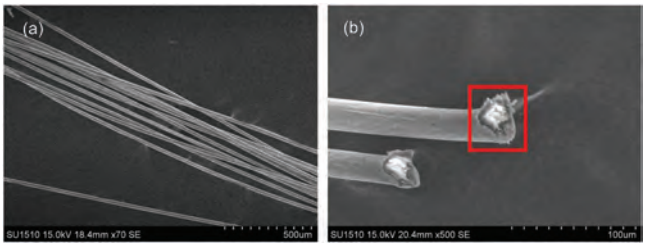

Figure 1. a) Side view of the silver fibre yarn. b) Cross-sectional view of the silver fiber yarn. For the cross-section in the red square the silver coating appears to be ≈4 to 5 µm thick.

2.1. Characterization of Core-Spun Yarns

Cotton fibers wrapped the silver fibers tightly, with the aid of polyurethane adhesive, forming a dense coating layer. The silver fibers are arranged closely in the center of core-spun yarn without exposure to the outside. **Figure 2**a,b show SEM images of the side and cross section views of the core-spun yarn before straining, with the EDS image in 2b indicating that the silver elements are localized within the yarn, where they are isolated by cotton fibers. Figure S1, from the Supporting Information, shows that the maximum elongations of the sensor caused by movements of knuckle, elbow, or knee, are not more than 14%. While under strain, or after 10 000 repeated 15% strain stretch-bend cycles (cycling rate 40 cycles/minute), the core-spun yarn maintains its coating fiber layer, which is shown in Figure 2c,d. The well maintained coating layer provided a robust dielectric layer, and ensured that the silver fibers were insulated from each other (resistance between fibers >2 MΩ). The good durability of the coating layer is chiefly due to the polyurethane adhesive spray-coated on the surface. Polyurethane adhesives have been widely used in bonding of textiles,[42,43] due to their elasticity and flexibility. They contain a large number of strong polar groups (-NHCOO- and -NCO), which are expected to enhance the adhesion between fibers. As shown in Figure 2e, the polyurethane adhesive coated the silver fibers well, and the coated fibers could withstand 20% strain without breaking. Ultimate strain was measured as ≈30% elongation (see Figure S2, Supporting Information). In addition, the ultimate loads of the core-spun yarns are higher than that of silver fiber yarns (see Figure S2, Supporting Information). The increase in ultimate load is an indication that the adhesion between the silver fibers and coating fiber layer is stable.[15]

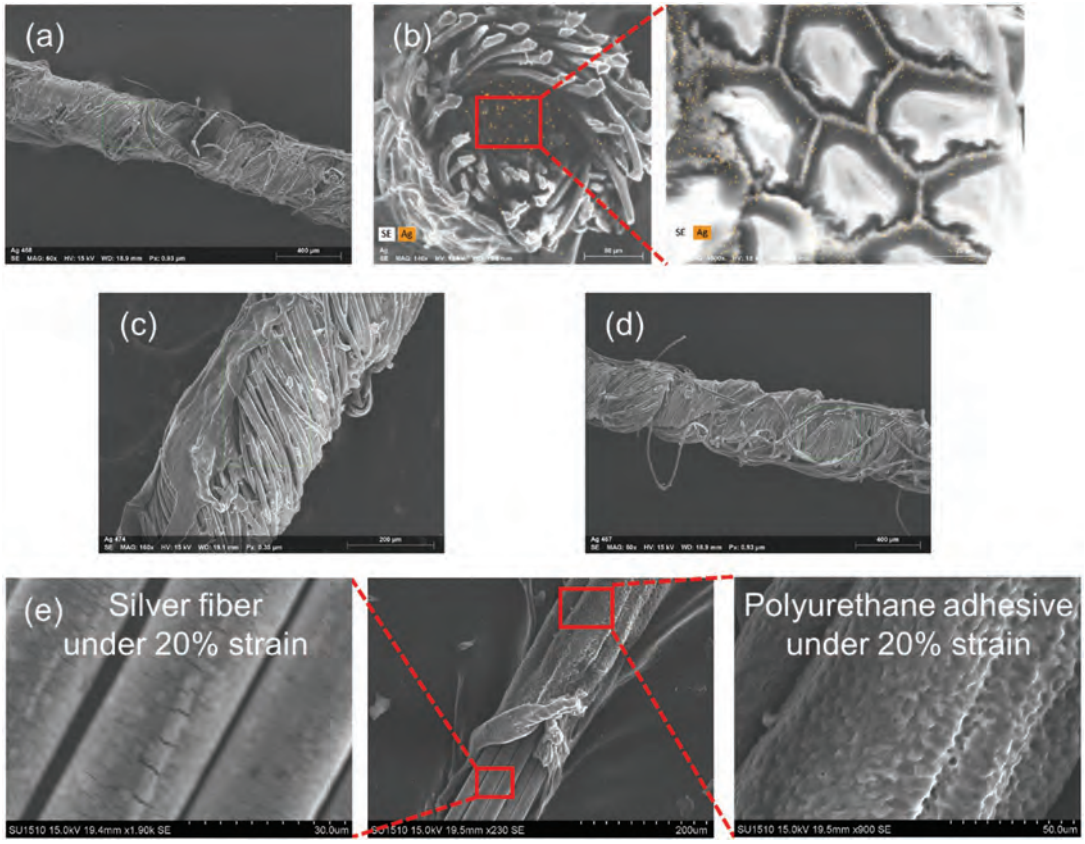

Figure 2. a) SEM side view image of the core-spun yarn before straining. b) SEM and EDS cross sectional view images of the core-spun yarn before straining. The SEM images reveal that the cotton fibers wrapped the silver fibers tightly, forming a dense coating layer which can obscure the silver elements. The EDS image indicates silver coating localization inside the core- spun yarn. c) SEM image of the side view of core-spun yarn under 15% strain. d) SEM image of the side view of core-spun yarn after 10 000 repeated stretch-bend cycles. e) SEM images of silver fibers coated with polyurethane adhesive under 20% strain. The corresponding higher magnification images show the surfaces of silver fibers as well as polyurethane adhesive coated on them, illustrating that the polyurethane adhesive can undergo 20% elongation without significant rupture.

Additionally, all the materials used are suitable for sterilization by gamma irradiation, or ethylene oxide treatment—the most common methods used for medical consumables.

2.2. Characterization of Double-Ply Yarn Strain Sensors

Double-ply yarn strain sensors were fabricated by twisting two core-spun yarns together, and fixing them with polyurethane adhesive, giving a double-helix capacitor structure. This capacitive sensor configuration is shown schematically in **Figure 3**a: the silver fibers are used as electrodes, with their cotton coating and the spray-coated polyurethane adhesive between them used as dielectric layers. According to Equation (1), their sensing mechanism is as follows: when the double-ply yarn sensor is stretched, the distance between two core-spun yarns (d) reduces and the area of electrodes (A) increases, resulting in a significant increase in capacitance. Micrographs and macro photographs of double-ply yarn sensors are shown in Figure 3. The double-ply yarn is fine in diameter (0.6 ± 0.05 mm), enabling use of typical sewing needles (Figure 3b). These new sensors can be embedded into cloth fabric by means of knitting, sewing, or weaving, as shown in Figure 3c. Apparent skin feel of the fabric was little changed, due to the softness of the double-ply yarn. Figure 3d,e shows the double-helix capacitor structure before straining, and Figure 3f–h shows its maintenance under strain, or after 10 000 repeated 15% elongation stretch–bend cycles. In addition, the ultimate load before failure of the double-ply yarn is double that of single fiber core-spun yarn (see Figure S3, Supporting Information)—this doubled ultimate load indicates that adhesion between the two twisted core-spun yarns is stable, and not limiting. Ultimate strain was ≈34% (Figure S3, Supporting Information), and elastic limit ≈18.5% elongation. The polyurethane adhesive spray-coated on the core-spun yarns contributed to its stable capacitor structure, playing two roles: a) in the mechanical aspect, the polyurethane adhesive provided a robust double-helix structure due to the adhesive strength of its bond with the fibers; and b) in the electrical aspect, the polyurethane adhesive filled in the clearance between the two twisted core-spun yarns to act as a partial dielectric (see corresponding higher magnification image in **Figure 4**c), providing a stable dielectric layer.

Silver fibers are promising materials for smart clothing due to their flexibility and antibacterial properties. Figure 4a–c shows the resistive strain sensor performance of the 10 cm long silver fiber yarn used in this study. The sensing mechanism is

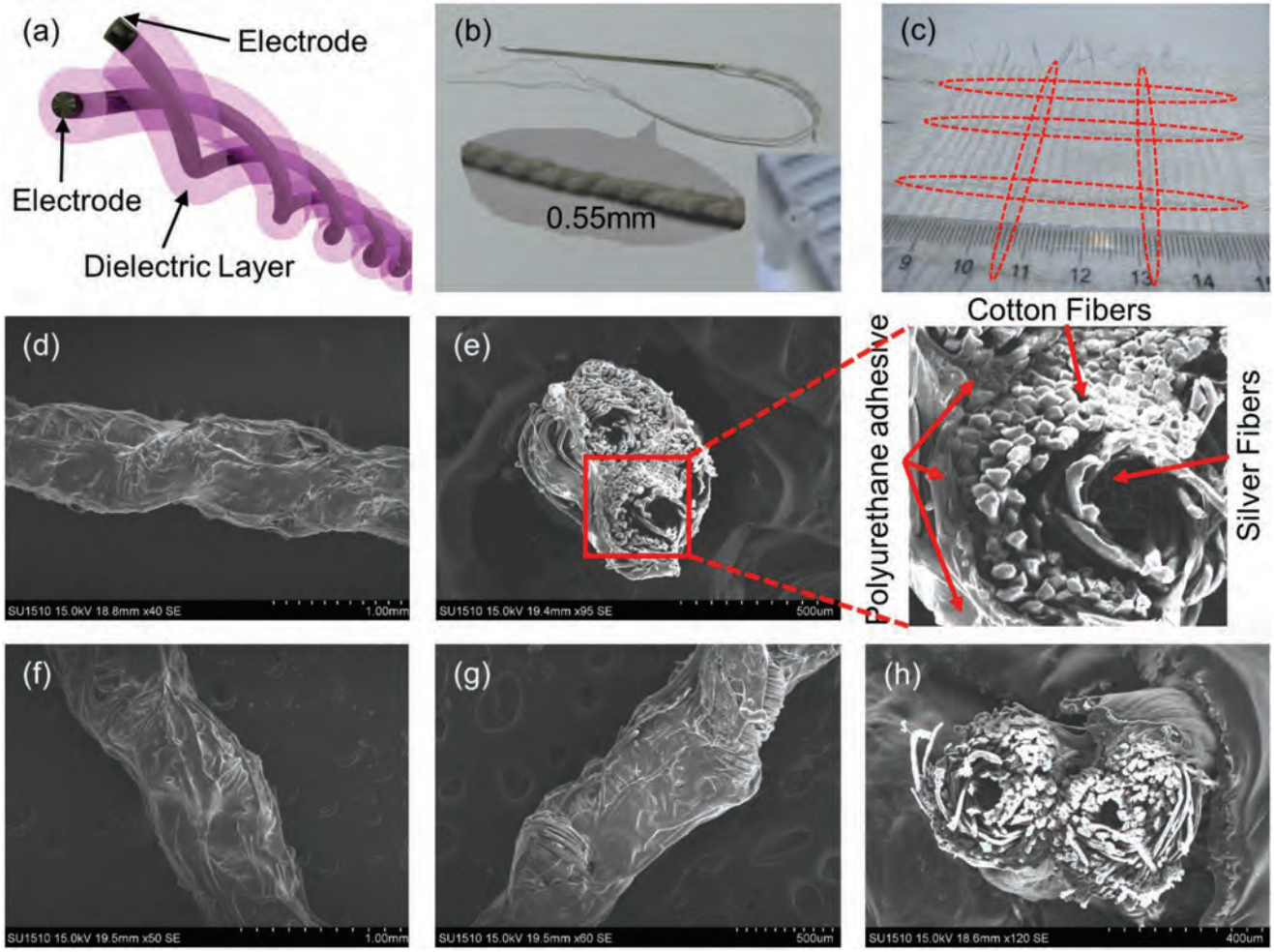

Figure 3. a) Schematic diagram of the double helix capacitor structure of double-ply yarn sensor. b) Macroscopic side and cross-sectional views of double-ply yarn sensor. c) The double-ply yarn sensors are knitted into fabrics by hand in this study. d,e) SEM images of the side and cross-sectional views of the double-ply yarn sensor before straining. The corresponding higher magnification image showed that polyurethane adhesive filled in the clearance between the two twisted core-spun yarns. f) SEM image of side view of double-ply yarn sensor under 15% strain. g,h) SEM images of the side and cross-sectional views of double-ply yarn sensor after 10 000 repeated stretch–bend cycles.

as follows: external strains cause the generation and expansion of cracks in the silver coating, as shown in Figure S4 in the Supporting Information, which leads to rupture of conductive paths, resulting in significant increases in resistance. Figure 4a shows obvious hysteresis in a single stretch–release cycle, typical of many resistive sensors.[2,18–24] Here this indicates that the cracks fail to recover completely with removal of external strain. The durability and stability of the silver fibers was investigated through repeated 15% elongation stretch–bend cycling tests. After 1000 cycles of stretching and bending, many cracks were not recovered 24 h after removal of external force (see Figure S5 in the Supporting Information). As the number of unrecoverable cracks increases further, the electrical paths become more and more "fragile," leading to dramatic drifts in sensitivity (revealed from the resistive gauge factor, which is defined as $(\Delta R/R)/\varepsilon$, where R is the resistance and ε is the mechanical strain).[44] This is shown for this system in Figure 4b. The strain-free resistance of the silver fibers increases rapidly versus number of cycles due to accumulation of broken conductive paths in the silver coating (Figure 4c). As mentioned above, these issues also exist in other wearable resistive sensors.[2,5,6,20–22,24] Their poor stability and high hysteresis restrict their use as resistive sensors.

By contrast, the capacitive sensing performance is stable and reliable when the silver fibers are used as the electrodes of the double-ply yarn sensor (10 cm long). Figure 4d shows negligible hysteresis in a single stretch–release cycle. From Figure 4e, we see that the double-ply yarn sensor exhibits an excellent linear relationship between capacitance and strain, and can detect strains below 1%. Based upon low-range 3σ estimation, limit of detection is ≈0.5%. As with the resistive sensing gauge factor, a capacitive strain gauge factor can be defined as the relative change in capacitance divided by the mechanical strain.[31,32] The capacitive strain gauge factor, g, is given by

$$g = \frac{\Delta C}{C\varepsilon} \tag{2}$$

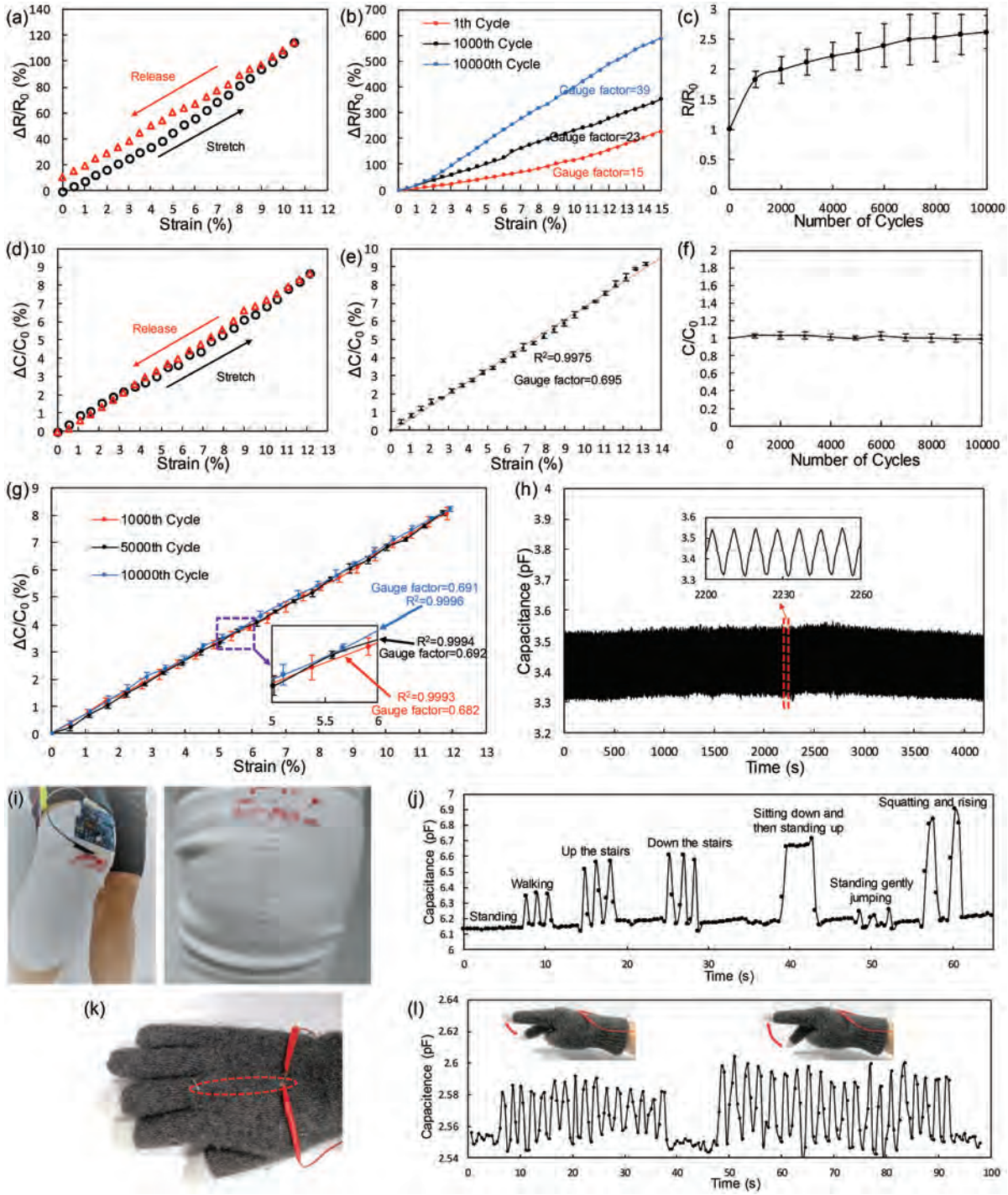

Figure 4. Sensing characteristic tests for silver fiber yarns and double-ply yarns. a) Relative resistance change of the silver fiber yarn from a single stretch–release cycle of strain at a uniform rate of 1% per second. b) Relationship between relative change in resistance and strain of silver fiber yarns after different numbers of repeated stretch–bend cycles. c) Relative strain-free resistances of silver fiber yarns versus number of repeated stretch–bend cycles. d) Relative change in capacitance of the double-ply yarn from a single stretch–release cycle of strain at a uniform rate of 1% per second. e) Relationship between relative change in capacitance and strain of double-ply yarns before repeated stretch–bend cycles. f) Relative strain-free capacitance of double-ply yarns versus number of repeated stretch–bend cycles. g) Relationship between relative change in capacitance and the strain of double-ply yarns after different numbers of repeated stretch–bend cycles. h) Capacitive response of the double-ply yarn sensor to repeated stretch–release cycles under a 10% strain at a rate of ≈2.2% per second. i) The double-ply yarn strain sensor was sewn into a kneepad and connected to a portable measuring circuit based on a capacitance measuring chip. j) The measured capacitance from the sensor-integrated kneepad undergoing various motions. k) The double-ply yarn strain sensor was sewn into a glove. i) The measured capacitance from the sensor-integrated glove during finger wiggling motions. Error bars represent the standard deviation of the repeated measurements.

When compared to reported capacitive systems, both gauge factor and limit of detection were similar. Relative to resistive type sensors, capacitive type sensors exhibit a lower sensitivity, as mechanical behavior and sensing mechanism limit their gauge factor to the order of 1.[31] Accordingly, the gauge factor of the double-ply yarn sensor (0.695) was considerably lower than for the silver fiber resistive sensor (15 to 39), but comparable to the typical range for capacitive sensors, 0.7 to 1.0. However, many of these capacitive systems demonstrated their characteristics over strains of 50% or more, which is more challenging for maintaining sensitivity and linearity than the 12% to 15% strains reported here. The comb-shaped, textile-silicone capacitive strain sensor reported by Atalay[35] had a higher gauge factor of 0.83, with a detection resolution of 1.36%. Comparisons with the performance of several representative polymer-based capacitive strain sensors can be made as follows: the sensor with a silver nanowire network of electrodes, and PDMS as dielectric, reported by Xu and Zhu,[30] claimed a gauge factor of ≈1, and strain limit of detection <1%. Yao and Zhu[31] developed a sensor with silver nanowires as electrodes, and Ecoflex as dielectric, which had a gauge factor of 0.7, and strain limit of detection <1%. Finally, a sensor with sprayed carbon nanotube (CNT) films as electrodes and Ecoflex as dielectric, reported by Lipomi et al.,[32] had a gauge factor of 0.4, and was not sensitive enough to detect strains less than 10%. Characteristics of comparable capacitive strain sensors are summarized in **Table 1**.

As shown in Figure 4f,g, there is no obvious detrimental effect on the capacitance from repeated 15% elongation stretch–bend cycling tests. Despite intensive cycling tests that involved 10 000 repeated cycles, the gauge factor, and strain-free capacitance of the double-ply yarn remained stable. In contrast, textile-based resistive strain sensors generally suffer from a drifting gauge factor and strain-free resistance in strain cycling tests.[2,5–7,10,19,20] Further, many reported textile-based strain sensors did not undergo strain cycle testing on the order of cycles reported here.[2,5,7,20,35] Again, many of these systems demonstrated their characteristics over strains of 50% or more, which is more challenging for sensor durability. Figure 4h shows that the measured capacitance of a double-ply yarn sensor undergoing repeated stretch–release cycles (under 10% strain) was stably maintained during cycling. This stability is mainly due to the stable dielectric structure, as stated earlier. Additionally, although conductive paths were broken during repeated strain cycling, the resistance of silver fiber stays the same order of magnitude as its initial value (range of resistance ≈172 to 450 Ω, as shown in Figure S6 from the Supporting Information). This demonstrates that the silver fibers are still good conductors, and are able to function as effective electrodes.

The capacitance of a 10 cm long double-ply yarn sensor was 3 to 4 pF. From the response time formula for a resistive-capacitive circuit[35] ($\tau = RC$, where τ is time constant, R is sensor-electrode resistance, and C is sensor capacitance), the time constant for the sensor was estimated to be on the order of several nanoseconds. This low time constant indicates a fast charge-discharge rate, enabling a short response time for the double-ply yarn sensor. However, response time is limited by other system components, and particularly by the sampling rate of the data acquisition system. Limited by the latter, response times were estimated by linear interpolation at ≈110 to 230 ms, as shown in Figure S7 from the Supporting Information. Typically, response times of ≈50 to 100 ms were reported in the literature.[22,32] Finally, relative change in strain-free capacitance was measured from 20% to 80% relative humidity (RH) at 24 °C (Figure S11, Supporting Information), with an ≈8% increase in capacitance over this range.

Table 1. Summary of published comparable capacitive strain and pressure sensor characteristics.

Material	Type of sensor	Measured	Gauge factor/sensitivity	Detection limit	Ref.
Silver fiber	Resistive	Strain	15–39	≈1%	This work
AgNW/PDMS-PDMS	Capacitive	Strain	≈1	<1%	[30]
AgNWs-Ecoflex	Capacitive	Strain	0.7	<1%	[31]
CNT film-Ecoflex	Capacitive	Strain	0.4	>10%	[32]
AgNW/PU-Acrylic elastomeric dielectric spacer	Capacitive	Strain	0.5	>1	[33]
Conductive fabric-Ecoflex	Capacitive	Strain	0.83	1.36%	[35]
Conductive PDMS-Ecoflex	Capacitive	Strain	0.55		[49]
Silver fiber-Cotton fiber	Capacitive	Strain	0.695	~0.5%	This work
Conductive rubber-Carbon black/silicone rubber dielectric	Capacitive	Pressure	0.2536 MPa^{-1} in the range up to 700kPa		[13]
AgNWs-Ecoflex	Capacitive	Pressure	0.00162 kPa^{-1} and 0.57 MPa^{-1} in below and above 500 kPa		[31]
CNT film-Ecoflex	Capacitive	Pressure	0.23MPa^{-1} in the range up to 1MPa	≈50kPa	[32]
AgNW/PU-Acrylic elastomeric dielectric spacer	Capacitive	Pressure	0.51MPa^{-1} in the range up to 1MPa	≈20kPa	[33]
Conductive fabric-Microporous silicone elastomer	Capacitive	Pressure	0.0121 kPa^{-1} in the range up to 100kPa	0.86 kPa	[46]
Conductive PDMS-Ecoflex	Capacitive	Pressure	0.417MPa^{-1} in the range up to 1.2MPa	50kPa	[49]
Silver fiber-Cotton fiber	Capacitive	Pressure	0.039711 kPa^{-1} below 0.85 kPa, 0.01922 kPa^{-1} below 35 kPa, 0.701 MPa^{-1} above 35 kPa	3.6Pa	This work

The double-ply yarn strain sensor was sewn into a kneepad as shown in Figure 4i. The subject wearing the monitoring device did not feel any restriction of movement. In basic human motion, each knee bends and bulges, leading to stretching of the kneepad device. Although it was made with one sensor, the kneepad could easily detect and distinguish various motions related to the flexion of the knee, including standing, walking, jumping, squatting, rising, sitting down and standing up, and also walking up and down stairs (see Figure 4j). Running was also monitored (Figure S10, Supporting Information). Another use case was detection of finger motion in a glove, where the sensor was again sewn into the clothing item. Capacitance was recorded when the middle finger was wiggled quickly up and down. The higher flexion-angle motion of finger bending was also recorded, and is given in Figure S9 in the Supporting Information. Due to the small amplitude rapid movements (≈1 Hz) of the knuckle, the sensor was required to be highly sensitive. Figures 4k clearly shows the individual finger movements. Slight differences in finger movement amplitude were also reflected in the capacitance record. It should be pointed out that the motion resolution is constrained by the sampling frequency (2 Hz) of the measurement circuit, rather than the inherent response characteristics of the double-ply yarn sensors.

The ultimate strain for the double-ply yarn sensor was ≈34% (Figure S3, Supporting Information), with elastic limit of ≈18.5%, while the maximum strain it suffered during use of wearable items was ≈14% (Figure S1, Supporting Information), well within these limits. Although typical skin strains of up to 44.6% have been reported for the knee joint during flexion,[45] clothing, and other fabrics items, may not suffer the full range of deformation the skin experiences, due to incomplete fixture to the skin. Additionally, the sensor can be integrated such that it comprises only a small fraction of wearable product fabric. Hence, the limits of elastic deformation for the sensor have not limited its use in detecting human motion, nor restricted its wearability.

2.3. Characterization of Textile-Based Capacitive Pressure Sensors

The core-spun yarns can also be woven into textile-based capacitive pressure sensors with a square-cross structure, as shown in **Figure 5**a. Capacitance is developed at the cross point of the core-spun yarns. External pressure reduces the distance between neighboring yarns, leading to an increase in capacitance. Critically for wearable sensors, the array of textile-based capacitive pressure sensors is well integrated into fabrics through weaving, which is shown in Figure 5b,c. Fabrics incorporating sensor arrays show no obvious detrimental effects on permeability and softness, and have potential antibacterial properties due to the fibers' silver coating.

Figure 6a presents the capacitive sensing characteristics of a textile-based pressure sensors array (1.0 cm by 0.7 cm in area). The sensor can withstand pressures of 200 kPa or more (maximum compression limit was not obtained due to restrictions of the texture analyzer). The sensitivity of the capacitive pressure sensor, S, can be defined as the slope of the traces in Figure 6a.

$$S = \frac{\delta\left(\frac{\Delta C}{C_0}\right)}{\delta p} \tag{3}$$

Here, p is the applied pressure, and C and C_0 are the capacitances with and without the applied pressure, respectively.

The sensitivity decreases with increasing pressure, in line with results consistently reported in the literature.[12,31,46,47] For pressures below 0.85 kPa and between 0.85 and 35 kPa, the sensitivities are 0.039711 and 0.01922 kPa^{-1}, respectively. Above 35 kPa sensitivity is 0.701 MPa^{-1}. The sensitivity in the low-pressure range is higher than many previously reported textile-based[11–14] and polymer-based[31–33,46–49] capacitive pressure sensors. For example, a sensor based on a textile substrate with carbon black/silicone rubber composite dielectric, reported by Guo et al.,[13] exhibited a sensitivity of 0.0002536 kPa^{-1} in the range up to 700 kPa. A sensor with conductive fabric as electrodes and microporous silicone elastomer as dielectric, reported by Atalay et al.,[46] exhibited a sensitivity of 0.0121 kPa^{-1} in the range up to 100 kPa. For pressures below and above 500 kPa, a sensor with silver nanowires as electrodes and Ecoflex as dielectric, reported by Yao et al.,[31] exhibited sensitivity of 0.00162 kPa^{-1} and 0.57 MPa^{-1}, respectively. Characteristics of comparable capacitive pressure sensors are summarized in Table 1.

As expected, sensitivity was highest for lowest applied pressures, with 0.33637 kPa^{-1} when the pressure was below 0.1 kPa. Based upon low-range 3σ estimation, limit of detection for this system was ≈3.6 Pa. From this level of sensitivity, the sensor array could reliably detect the loading and unloading of a single soybean (≈200 mg), as shown in Figure 6b. Figure 6c

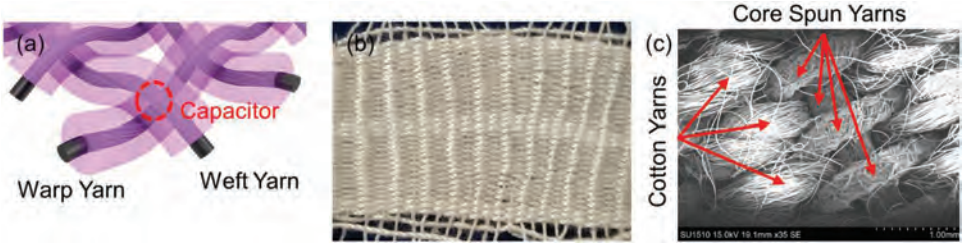

Figure 5. a) Schematic diagram of the array of textile-based capacitive pressure sensors. bc) Macro photograph and SEM micrograph of the 880 µm thick array of textile-based capacitive pressure sensors integrated in fabrics. The lower color intensity fibers in (b) are the sensor core-spun yarn fibers.

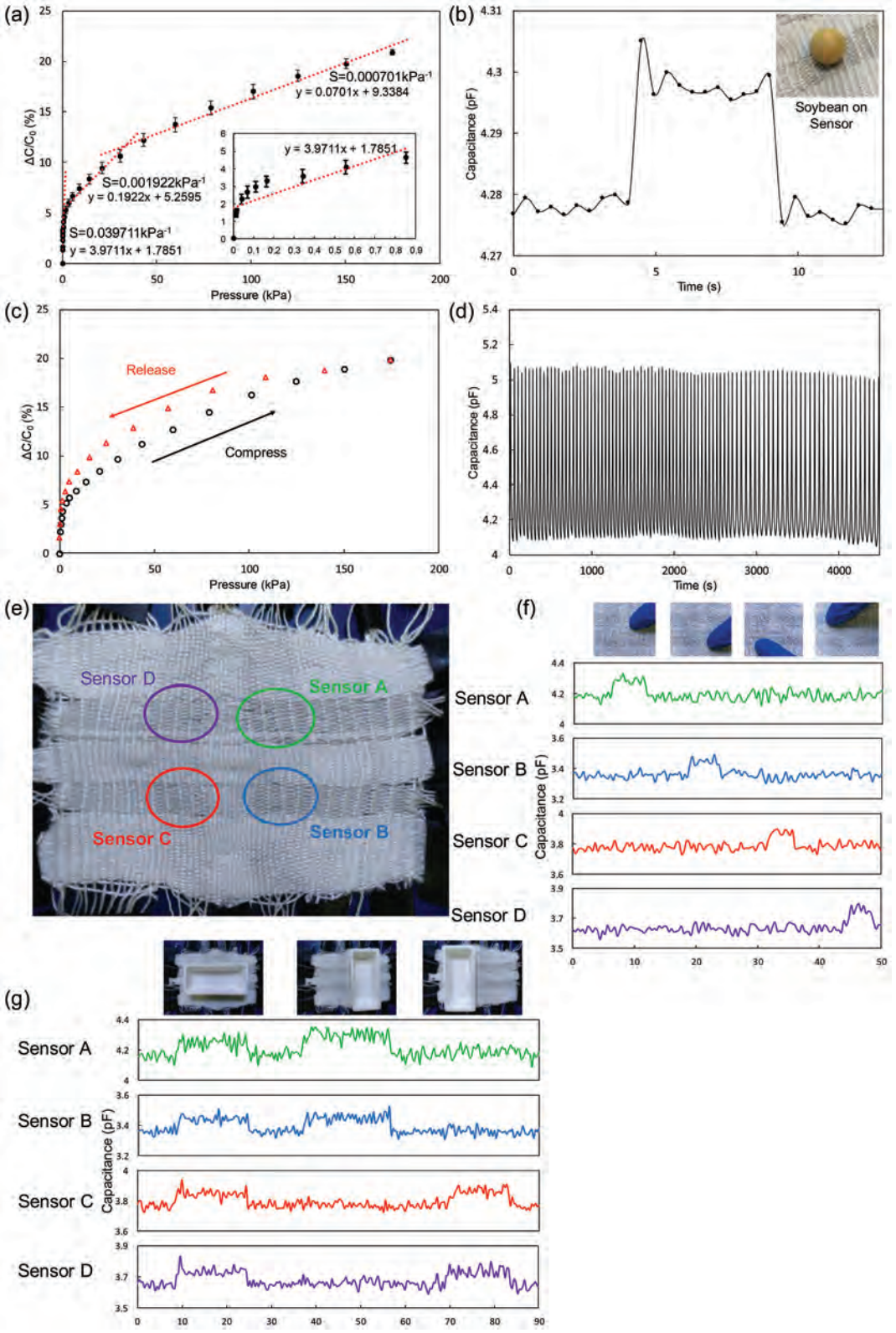

Figure 6. a) Relationship between relative change in capacitance and applied pressure of the array of textile-based pressure sensors. b) Capacitive response of the sensor array to the loading and unloading of a soybean (≈200 mg). c) Capacitance change of the sensor array during a single compress-release cycle of compression. d) Capacitive response of the sensor array to repeated compress–release cycles under a pressure of 200 kPa. e) Four sensor arrays were woven into a mat. f,g) Simultaneously measured capacitances from the four sensor arrays, while fingers or weighing boats were rested upon them. Error bars represent the standard deviation of the repeated measurements.

shows the capacitive change of the sensor array from a single compress–release cycle of compression. A slight hysteresis was observed in the compress–release cycle, similar to the "negligible" amount reported by Lee.[15] As shown in Figure 6d, the sensor array exhibits stable output signals in repeated compress–release cycles under a pressure of 200 kPa. Four sensor arrays were woven into a mat, as shown in Figure 6e. The mat can measure pressure from four positions simultaneously. As shown in Figure 6f,g, the positions where fingers were pressed, or a porcelain combustion boat was rested, were clearly determined. The fine fibers of the sensor material could enable the incorporation of large numbers of sensors into devices, but this capability may be limited by capacity for multiplex detection of data acquisition systems, rather than sensor size.[50]

2.4. Characterization of Fabric Bacterial Resistance

The textile sensors have potential antibacterial properties due to the silver coating in the core-spun yarns. Samples of the sensor array-integrated fabrics prevented growth of bacteria in a shaker flask culture. This is shown in Figure S12b in the Supporting Information, by the failure of the flask media to produce bacterial colonies when inoculating a culture plate. After wearing or washing, it still maintains this property, as shown in Figure S12c,d in the Supporting Information. Further examination will be required, where devices are assessed immediately after wearing, as the polyurethane adhesive may prevent the transport of water molecules and silver ions required for antibacterial action. It may be that the sensor material can only potentially exhibit antimicrobial properties when it is exposed to sweat, or it is being washed. Accordingly, wetting behavior of the material should also be assessed.

3. Conclusions

The first effective, matrix-free, textile-only capacitive strain sensor was developed. It was fabricated by twisting two core-spun yarns into a double-helix double-ply yarn, giving it a fine diameter (0.6 ± 0.05 mm) and the morphology of fabric thread. This form enables facile integration, via weaving or sewing, with clothing, athletic accessories, and medical products such as bodily supports and bandages. Elastic limit was measured as ≈18.5% elongation, with ≈34% ultimate strain.

The individual core-spun yarns were fabricated by wrapping silver-coated nylon fibers with cotton fibers, and fixing with polyurethane adhesive. The double-ply yarn sensor possessed a robust dielectric layer, and due to this stable capacitance, it displayed excellent linearity ($R^2 = 0.9975$), as well as low hysteresis and high stability over more than 10 000 repeated bend-stretch cycles (15% elongation). Few reported sensors have been subjected to this degree of endurance testing. Gauge factor (0.695) and detection limit (≈0.5%) were in line with existing systems, when tested up to 15% strain. However, many published capacitive sensors were characterized over 50% or higher strains, which is more challenging for linearity and durability.

Response time was estimated between 110 and 230 ms, but characterization was limited by available apparatus (500 ms sampling period), and further characterization may be desired. Ease of integration of the sensor was demonstrated by sewing into kneepads and gloves. The full range of subjects' motions were clearly distinguished, and subjects did not feel any discomfort or restriction of movement, even during high flexion-angle motions. All materials are suitable for sterilization via gamma irradiation or ethylene oxide treatment, enabling the sensor's use in aseptic medical products.

The core-spun yarn was also woven into a capacitive type of matrix-free, textile-based pressure sensor, by stacking the two core-spun yarns perpendicularly to each other. An array of these sensors is easily integrated into fabrics via weaving. These pressure sensors displayed good sensitivity (0.039711 kPa^{-1} below 0.85 kPa, 0.01922 kPa^{-1} between 0.85 and 35 kPa, and 0.701 MPa^{-1} above 35 kPa), stable capacitance over 500 cycles, and have the potential for antibacterial properties (assessed according to Chinese Standard GB/T 20 944.3-2008). Sensors were blended into wearable fabrics, and mats for motion detection, demonstrating wide applicability. Again, subjects did not feel any restriction of movement or discomfort

The sensors presented here possess an attractive combination of ease of fabrication and integration, enabling new potential in versatility and comfort, without restrictive cost. Together with their performance and durability, antibacterial properties, and sterilizable materials, they have much commercial and scientific promise as wearable sensors, particularly for smart clothing and medical products. Currently they are limited to applications where direct 1:1 measurement of large skin strains is not required, due to their degree of extensibility. Future development may include optimization of the fiber core material, to remove this limitation.

4. Experimental Section

Fabrication of Core-Spun Yarns: The sensors from this study were fabricated via the process shown in **Figure 7**. Silver-coated nylon core (Nylon 6 partially oriented yarn) fibers (0.07 mm diameter, Zhi Yuan Xiang Yu Ltd., Qing Dao City, China) were wrapped with cotton fiber yarn (0.15 mm), spray coated with one-component polyurethane adhesive (Yue Cheng Adhesive Factory, Yi Wu City, China), and dried with a hot air dryer. As shown in Figure 7, the cotton fibers that were wrapped on the surface provided an insulation layer, with the silver fibers used as a conductive inner core.

Fabrication of Double-Ply Yarn Sensor: Two core-spun yarns were twisted into a double-ply yarn, giving it a double helix capacitor structure. The double-ply yarn was then sprayed with polyurethane adhesive. After drying of the adhesive, the new sensor, with double helix capacitive structure, was ready. Sensors were sewn into the proof-of-principle items (kneepads and gloves) by hand with a sewing needle. The items were worn and tested by the researcher, and no institutional review or consent documents were required.

Fabrication of Array of Textile-Based Pressure Sensors: Two reels of core-spun yarns were used as the weft and warp yarns. Then the wearable fabric array of textile-based pressure sensors was formed by interlacing the weft and warp yarns with cotton thread on a loom.

Characterization: Morphological characterization in this study was carried out with a Hitachi SU1510 (Hitachi High-Technologies Corporation, Japan) SEM. A Bruker energy dispersive spectrometer (XFlash 6130, Bruker Corporation, USA) connected to the microscope was employed to observe element distribution on surfaces. Tensile fracture tests were carried out on a texture analyzer (Brookfield CT3 50K, AMETEK Brookfield, USA) at a test speed of 0.5 mm s^{-1}. The pressure testing was also carried on this texture analyzer. Capacitances

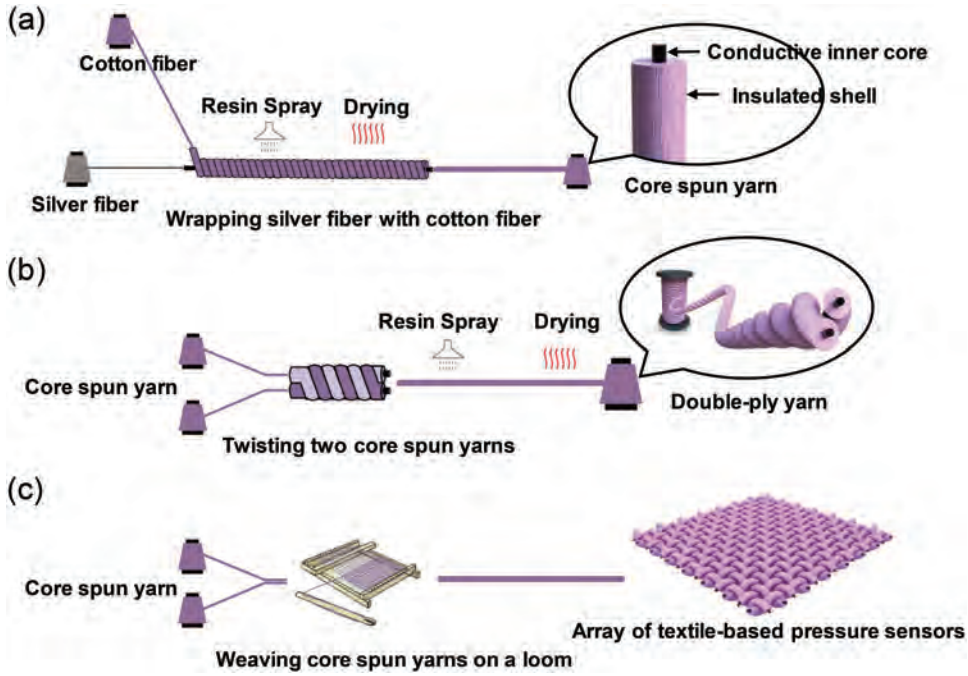

Figure 7. Fabrication process for double-ply yarn sensors, and the array of textile-based pressure sensors. a) Fabrication of core-spun yarns by wrapping cotton around silver coated nylon core fiber, followed by application and drying of polyurethane adhesive resin. b) Fabrication of double-ply yarn sensor by twisting two core-spun yarns into a double-helix capacitive structure, followed by application and drying of polyurethane adhesive resin. c) Fabrication of array of textile-based pressure sensors by weft and warp weaving of two core-spun yarns.

of sensors were measured with a capacitance meter (TH2638, Tong Hui Ltd, Chang Zhou City, China), or a portable measuring circuit based on a capacitance measuring chip (PCAP01, Acam-Messelectronic Gmbh, Germany), at a sampling rate of 2 Hz. The tensile strain testing and stretch–bend cycling endurance testing were carried out on a custom-made tensile testing machine. For the latter, 15% was the maximum elongation, with cycling rate of 40 cycles/minute.

Bacterial Resistance Test: E. coli (ATCC29522) was selected as the model species for characterizing sensor fabric bacterial resistance. Antibacterial activity was assessed in accordance with the shake flask test from the Chinese Standard GB/T 20 944.3-2008[51,52] (Textiles—Evaluation for antibacterial activity—Part 3: Shake flask method). 0.75 g of each fabric sample (pure cotton cloth, unused sensor array-integrated fabric, subject worn sensor array-integrated fabric, washed sensor array-integrated fabric) was cut into small pieces of dimensions around 5 × 5 mm^2, which were sterilized for 15 min at 103 kPa (gauge) and 125 °C in an autoclave. A fresh bacterial suspension was first acquired by culturing *E. coli* in 20 mL of autoclaved broth (3 g L^{-1} beef extract, 5 g L^{-1} peptone, Sinopharm Chemical Reagent Ltd., China), in a 500 mL conical flask, at 37 °C for 20 h after inoculation at 130 rpm shaking rate. Subsequently, 2 mL of the bacterial suspension was removed and diluted in autoclaved broth and buffer solution (PBS, 0.03 mol L^{-1}, pH = 7.2–7.4) to reach a concentration of ≈3×10^5 CFU mL^{-1} for the sterilization test. Then 5 mL of the diluted bacterial solution was placed into an autoclaved 500 mL conical flask (containing 0.75 g of sample and 70 mL of PBS) at 24 °C for 18 h; at 150 rpm shaking rate. Finally, 1 mL of the bacterial solution from the conical flask was spread evenly on agar dishes (3 g L^{-1} beef extract, 5 g L^{-1} peptone, 15 g L^{-1} agar, Sinopharm Chemical Reagent Ltd., China), and incubated for 24 h at 37 °C. Photographs of colonies on the surface of dishes were taken with a colony counter (Czone 5F, Shineso Ltd., Hang Zhou City, China). The subject wore the sensor array-included fabric as follows: a piece of the fabric with dimensions ≈3 cm × 8 cm was secured to the subject's arm, using tape to ensure contact with skin, 4 h per day for a month. The items were worn and tested by the researcher, and no institutional review or consent documents were required. The sensor array-integrated fabric was washed ten times using the following scheme: an ≈5 cm × 5 cm piece of the fabric was soaked in water containing laundry detergent for 10 min, then flushed with deionized water for 5 min, and was finally dried in a vacuum oven at 40 °C for 24 h.

Supporting Information

Supporting Information is available from the Wiley Online Library or from the author.

Acknowledgements

The authors would like to thank the School of Chemical and Environmental Engineering of the College of Chemistry, Chemical Engineering and Material Science, Soochow University, for funding this study, and for providing a partial Ph.D. scholarship for Q.Z.

Conflict of Interest

The authors declare no conflict of interest.

Keywords

capacitive strain sensors, human motion detection, smart clothing, textile sensors, wearable sensors

Received: June 9, 2019
Published online:

[1] S. D. Min, Y. Yun, H. Shin, *IEEE Sens. J.* **2014**, *14*, 3245.
[2] J. Eom, R. Jaisutti, H. Lee, W. Lee, J. S. Heo, J. Y. Lee, S. K. Park, Y. H. Kim, *ACS Appl. Mater. Interfaces* **2017**, *9*, 10190.
[3] R. M. Kwasnicki, R. Ali, S. J. Jordan, L. Atallah, J. J. Leong, G. G. Jones, J. Cobb, G. Z. Yang, A. Darzi, *Int. J. Surg.* **2015**, *18*, 14.
[4] S. Jcm, J. Barth, F. Marxreiter, J. Gossler, Z. Kohl, S. Reinfelder, H. Gassner, K. Aminian, B. M. Eskofier, J. Winkler, *PLoS One* **2017**, *12*, e0183989.
[5] B. C. Zhang, H. Wang, Y. Zhao, F. Li, X. M. Ou, B. Q. Sun, X. H. Zhang, *Nanoscale* **2016**, *8*, 2123.
[6] X. Wu, Y. Han, X. Zhang, C. Lu, *ACS Appl. Mater. Interfaces* **2016**, *8*, 9936.
[7] J. J. Park, W. J. Hyun, S. C. Mun, Y. T. Park, O. O. Park, *ACS Appl. Mater. Interfaces* **2015**, *7*, 6317.
[8] Y. Wang, L. Wang, T. T. Yang, X. Li, X. B. Zang, M. Zhu, K. L. Wang, D. H. Wu, H. W. Zhu, *Adv. Funct. Mater.* **2014**, *24*, 4666.
[9] S. Ryu, P. Lee, J. B. Chou, R. Xu, R. Zhao, A. J. Hart, S. G. Kim, *ACS Nano* **2015**, *9*, 5929.
[10] Z. Wang, H. Yan, J. Sun, H. Yang, H. Hong, R. Jiang, W. Gai, G. Li, C. Zhi, *ACS Appl. Mater. Interfaces* **2016**, *8*, 24837.
[11] T. Hoffmann, B. Eilebrecht, S. Leonhardt, *IEEE Sens. J.* **2011**, *11*, 1112.
[12] J. Meyer, B. Arnrich, J. Schumm, G. Troster, *IEEE Sens. J.* **2010**, *10*, 1391.
[13] X. Guo, Y. Huang, X. Cai, C. Liu, P. Liu, *Meas. Sci. Technol.* **2016**, *27*, 045105.
[14] S. Takamatsu, T. Kobayashi, N. Shibayama, K. Miyake, T. Itoh, *Sens. Actuators, A.* **2012**, *184*, 57.
[15] J. Lee, H. Kwon, J. Seo, S. Shin, J. H. Koo, C. Pang, S. Son, J. H. Kim, Y. H. Jang, D. E. Kim, *Adv. Mater.* **2015**, *27*, 2433.
[16] T. Q. Trung, N. E. Lee, *Adv. Mater.* **2016**, *28*, 4338.
[17] M. Amjadi, K. U. Kyung, I. Park, M. Sitti, *Adv. Funct. Mater.* **2016**, *26*, 1678.
[18] O. Atalay, W. R. Kennon, E. Demirok, *IEEE Sens. J.* **2015**, *15*, 110.
[19] Y. Cheng, R. Wang, J. Sun, L. Gao, *Adv. Mater.* **2015**, *27*, 7365.
[20] H. Zhang, X. M. Tao, T. X. Yu, S. Y. Wang, *Sens. Actuators, A* **2006**, *126*, 129.
[21] A. P. Sobha, S. K. Narayanankutty, *Sens. Actuators, A* **2015**, *233*, 98.
[22] L. Cai, L. Song, P. Luan, Q. Zhang, N. Zhang, Q. Gao, D. Zhao, X. Zhang, M. Tu, F. Yang, W. Zhou, Q. Fan, J. Luo, W. Zhou, P. M. Ajayan, S. Xie, *Sci. Rep.* **2013**, *3*, 3048.
[23] M. Amjadi, A. Pichitpajongkit, S. Lee, S. Ryu, I. Park, *ACS Nano* **2014**, *8*, 5154.
[24] C. X. Liu, J. W. Choi, *Microelectron. Eng.* **2014**, *117*, 1.
[25] D. Kang, P. V. Pikhitsa, Y. W. Choi, C. Lee, S. S. Shin, L. Piao, B. Park, K. Y. Suh, T. I. Kim, M. Choi, *Nature* **2014**, *516*, 222.
[26] M. Li, H. Li, W. Zhong, Q. Zhao, D. Wang, *ACS Appl. Mater. Interfaces* **2014**, *6*, 1313.
[27] R. Rahimi, M. Ochoa, W. Yu, B. Ziaie, *ACS Appl. Mater. Interfaces* **2015**, *7*, 4463.
[28] X. Liao, Q. Liao, X. Yan, Q. Liang, H. Si, M. Li, H. Wu, S. Cao, Y. Zhang, *Adv. Funct. Mater.* **2015**, *25*, 2395.
[29] D. J. Cohen, D. Mitra, K. Peterson, M. M. Maharbiz, *Nano Lett.* **2012**, *12*, 1821.
[30] F. Xu, Y. Zhu, *Adv. Mater.* **2012**, *24*, 5117.
[31] S. Yao, Y. Zhu, *Nanoscale* **2014**, *6*, 2345.
[32] D. J. Lipomi, M. Vosgueritchian, B. C. Tee, S. L. Hellstrom, J. A. Lee, C. H. Fox, Z. Bao, *Nat. Nanotechnol.* **2011**, *6*, 788.
[33] W. Hu, X. Niu, R. Zhao, Q. Pei, *Appl. Phys. Lett.* **2013**, *102*, 38.
[34] A. Atalay, V. Sanchez, O. Atalay, D. M. Vogt, F. Haufe, R. J. Wood, C. J. Walsh, *Adv. Mater. Technol.* **2017**, 2.
[35] O. Atalay, *Materials* **2018**, *11*, 768.
[36] A. Nag, R. B. V. B. Simorangkir, E. Valentin, T. Björninen, S. C. Mukhopadhyay, *IEEE Access* **2018**, *6*, 71020.
[37] L. M. Castano, A. B. Flatau, *Smart Mater. Struct.* **2014**, 23.
[38] W. Wang, W. Li, C. Gao, W. Tian, B. Sun, D. Yu, *Appl. Surf. Sci.* **2015**, *342*, 120.
[39] M. P. Gashti, S. T. Ghehi, S. V. Arekhloo, A. Mirsmaeeli, A. Kiumarsi, *Fibers Polym.* **2015**, *16*, 585.
[40] S. T. Dubas, P. Kumlangdudsana, P. Potiyaraj, *Colloid Surf.* **2006**, *289*, 105.
[41] S. H. Jeong, Y. Y. Sang, S. C. Yi, *J. Mater. Sci.* **2005**, *40*, 5407.
[42] K. H. Remley, Polyurethane textile adhesive. In US, **1977**.
[43] H. Stepanski, V. Nebe, *J. Ind. Text.* **1997**, *27*, 27.
[44] T. Yamada, Y. Hayamizu, Y. Yamamoto, Y. Yomogida, A. Izadi-Najafabadi, D. N. Futaba, K. Hata, *Nat. Nanotechnol.* **2011**, *6*, 296.
[45] A. M. Wessendorf, D. J. Newman, *IEEE Trans. Biomed. Eng.* **2012**, *59*, 3432.
[46] O. Atalay, A. Atalay, J. Gafford, C. Walsh, *Adv. Mater. Technol.* **2018**, *3*, 1700237.
[47] J. A. Dobrzynska, M. A. M. Gijs, *J. Micromech. Microeng.* **2013**, 23.
[48] Y. Ming, A. P. Bonifas, L. Nanshu, S. Yewang, L. Rui, C. Huanyu, A. Abid, H. Yonggang, J. A. Rogers, *Nanotechnology* **2012**, *23*, 344004.
[49] S. J. Woo, J. H. Kong, D. G. Kim, J. M. Kim, *J. Mater. Chem. C* **2014**, *2*, 4415.
[50] A. Nelson, G. Singh, R. Robucci, C. Patel, N. Banerjee, *IEEE Trans. Multi-Scale Comput. Syst.* **2015**, *1*, 62.
[51] D. Zhang, G. W. Toh, H. Lin, *J. Mater. Sci.* **2012**, *47*, 5721.
[52] X. Fu, Y. Shen, X. Jiang, D. Huang, Y. Yan, *Carbohydr. Polym.* **2011**, *85*, 221.